

Research article

Bioactive Profile Analysis and Inhibitory Activity of Prostaglandin Synthase from Sungkai Leaf Extract (*Peronema canescens* Jack) In Silico

Muhammad Marsha Azzami Hasibuan¹, Dimas Andrianto¹ and Raden Haryo Bimo Setiarto^{2*}

¹Department of Biochemistry, IPB University, Bogor, West Java 16680, Indonesia

²Research Center for Applied Microbiology, National Research and Innovation Agency (BRIN), KST Soekarno, Cibinong, Bogor, West Java, 16911, Indonesia

Received: 9 September 2024, Revised: 16 December 2024, Accepted: 2 January 2025, Published: 27 March 2025

Abstract

Sungkai leaves (*Peronema canescens* Jack) have antipyretic properties that have been proven ethnobiologically. However, research on sungkai leaves is scarce, especially in silico and in vitro. The aim of this study was to prove the ability of sungkai leaves to accelerate the process of decreasing body temperature during fever using the silico method. Sungkai leaves were extracted using a 70% ethanol solvent. The extract solution was concentrated using a rotary evaporator and then analyzed using an LC-MS device. Compounds obtained from the LC-MS analysis were screened in silico using Lipinski's rule of 5 and ADMET. The compounds that successfully passed the screening were docked with the target enzyme mPGES-1 using the Yasara Structure application. Extraction with 70% ethanol solvent resulted in an extract yield of 14.75%. The results of the LC-MS analysis showed the presence of 22 known compounds and one unknown compound. The screening results showed that ten compounds had successfully passed. Compounds 2-oxo-6-(piperidine-1-sulfonyl)-benzoxazole-3-carboxylic acid isobutyl ester; 2-(5-([Isopropyl (methyl)amino] methyl) - 1 - tetrazolidinyl) - N - methyl - N - [2 - (2 - methyl - 1 - imidazolidinyl) ethyl] acetamide; 2-([2-[4-(2-Hydroxyethyl)-1-piperazinyl]-2-oxoethyl] sulfanyl)-5,6-dimethylthieno[2,3-d]pyrimidin-4(3H)-one; 2-([4 amino -5-[3-(diethylsulfamoyl) phenyl]-4H-1,2,4-triazol-3-yl]sulfanyl)-N-dimethylacetamide; and 3, 4,5-trimethoxycinnamate obtained from this study could inhibit mPGES-1 based on the binding energy and inhibition constant that each test ligand had.

Keywords: bioactive; fever; LC-MS; molecular docking; sungkai

*Corresponding author: E-mail: haryobimo88@gmail.com

<https://doi.org/10.55003/cast.2025.264645>

Copyright © 2024 by King Mongkut's Institute of Technology Ladkrabang, Thailand. This is an open access article under the CC BY-NC-ND license (<http://creativecommons.org/licenses/by-nc-nd/4.0/>).

1. Introduction

Fever is one of the preliminary conditions in many diseases, and it is a normal body response against microorganism infection or environmental effects. Fever starts with an increase in body temperature to above the normal range (above 37°C). Fever may occur due to pyrogenic thermoregulators triggered by sepsis or inflammatory conditions (Walter et al., 2016). The purpose of the increase in body temperature is to protect the body via several mechanisms. Incoming pathogens that infect the body usually replicate well at 37°C. Thus, increasing body temperature helps inhibit pathogen replication. On the other hand, a body with a temperature above 40 °C can experience a side effect, such as death, because high temperature can damage organs and cellular functions in the human body (Walter et al., 2016).

Medications that treat fever usually use antipyretic compounds such as paracetamol (Carlson et al., 2019). Paracetamol is one of the drugs that can be used to treat fever and mild pain. Paracetamol works by inhibiting the mechanism of the prostaglandin H₂ synthase (PGHS) enzyme. PGHS has two active sites: cyclooxygenase (COX) and peroxidase (POX). The COX site transforms arachidonic acid into an intermediate compound hyperoxide and then into prostaglandin H₂ by the active POX site. Paracetamol inhibits the enzymatic activities of COX by reducing POX so that POX cannot accept electrons from the oxidation process of COX. Paracetamol inhibits POX regeneration while also inhibiting the formation of prostaglandins that increase body temperature (Sharma & Mehta, 2014). By inhibiting the formation of prostaglandins, the temperature of the body gradually decreases.

Paracetamol is included in drugs that are safe to consume, but it can cause drug overdose if consumed for a long time. This overdose is dangerous because it can cause hepatic cell necrosis in the centrilobular area, thus causing acute liver failure, and decreasing the level of glutathione-SH (GSH) in the liver, which causes liver cells to be exposed to oxidant damage. Moreover, N-acetyl-p-benzoquinone imine, a toxic metabolite of paracetamol, can cause enzymatic system failure (Rafita et al., 2016). Therefore, natural remedies that are safe and reliable are needed. One ethnobotanical endemic plant often used as medicine is the sungkai leaf (*Peronema canescens* Jack). Sungkai is classified as a woody plant that can grow to 20-30 m in length with a trunk diameter of 0.6 m. Sungkai grows well at an altitude of 0-600 masl in tropical weather (Rafita et al., 2016). Based on data uploaded on the website of the Ministry of Environment and Forestry of the Republic of Indonesia, sungkai trees are widely spread in Sumatra, Java and Kalimantan, to be precise in West Sumatra, Jambi, Bengkulu, South Sumatra, Lampung, West Java and throughout Kalimantan. This plant is used for traditional medicine by various tribes in Indonesia. The Dayak people use brewed sungkai leaves to treat fever, influenza, and stomach aches and as an antiseptic for the mouth and skin (Yani et al., 2014).

Sungkai leaves are used in ethnobiological ways as febrifuges and natural antibiotics by the people of the interior of Kalimantan. However, the profile of the bioactive components that act as antipyretics in sungkai leaves is still unknown. The public widely use paracetamol as a fever medicine in general, but it can have quite a significant impact if it is misused. This encourages the discovery of antipyretic compounds derived from natural ingredients that are safer when consumed. In this research, the bioactive compounds in sungkai leaf extract (*Peronema canescens* Jack) that specifically have a role as antipyretic fever reducers were identify using the liquid chromatography–mass spectrometry (LC-MS) method and the molecular docking in silico analysis approach.

2. Materials and Methods

2.1 Materials

Sungkai leaves taken from the Faculty of Forestry, Bogor Agricultural University collection, distilled water and 70% ethanol were used in this study. The equipment used for the analysis were glassware, rotary evaporator (LabTech Ltd.), micropipette (Dragonlab), HP Victus 16 Laptop, ACQUITY UPLC®H-Class System (waters, USA), ACQUITY UPLC® HSS C18 (1.8 µm 2.1x100 mm) (waters, USA), Xevo G2-S QToF (waters, USA), PerkinElmer ChemOffice 2017 software, YASARA Structure, Pymol, ChemAxon, Masslynx, and Discovery Studio Visualizer.

2.2 Methods

2.2.1 Extraction of sungkai leaves

The extraction process was carried out on fresh leaves using a maceration method of 70% ethanol solvent. Maceration was done by adding one part of the simplicial to the macerator with ten parts of solvent (1:10). Incubation was carried out for 24 h (soaked). The macerate obtained was then separated by filtration using a Buchner funnel to speed up filtering. The maceration process was repeated three times using the same amount and type of solvent. The maceration was concentrated using a rotary evaporator at the temperature of 50°C and rotation speed at 75 RPM to produce a thick extract. Furthermore, the yield value obtained was determined: the weight percent (w/w) of the extracts and the simplicial weight (Latief et al., 2021; Pindan et al., 2021).

2.2.2 Moisture content analysis

First, porcelain cups were dried in an oven at 105°C for 30 min, then cooled in a desiccator for 30 min. Each cup was then weighed on an analytical balance. Two grams of sample were added to the porcelain cup, and then weighed on an analytical balance and dried in an oven at 105°C for approximately 3 h, cooled in a desiccator and then weighed. This step was repeated 3 times (Irsal et al., 2022). Measurement of the moisture content was carried out three times and measured by the formula:

$$\text{Moisture content} = \left(\frac{M1 - M2}{M1} \right) \times 100\%$$

Where M1 = Sample weight before dried (g) and M2 = Sample weight after dried (g).

2.2.3 Bioactive compound profiling of sungkai leaves by LC-MS

Bioactive compound profiling of ethanol extract was performed using an ultra performance liquid chromatography–mass spectrometry (UPLC-MS). Each prepared sample (5µL) was injected into the UHPLC Vanquish Tandem Q Exactive Plus Orbitrap HRMS ThermoScientific instrument using a micro syringe, with the temperature set to 30°C and using two eluents, eluent (A): H₂O + 0.1% formic acid and eluent (B): acetonitrile + 0.1% formic acid. After that, raw data was obtained in the form of chromatograms and spectra for each sample, which were then processed with Masslynx software to obtain data on the

peak area, retention time, measured mass, calculated mass and the formula for each detected peak. Furthermore, data interpretation was carried out through the ChemSpider website and Chemdraw software to obtain the names and chemical structures of the compounds found to obtain metabolite profiles from Sungkai leaves (Hanafi et al., 2018).

2.2.4 Test of prostaglandin synthase inhibition as antipyretic in silico

PASS was in silico-based software that was used to analyze secondary metabolites of *Peronema canescens* Jack that had potential as antipyretics based on literature studies and several databases (Pubchem, KNApSAcK family databases, and Duke's Phytochemical and Ethnobotanical Databases), the ligands from said databases are then input to WAY2DRUG PASS on the website (<http://pharmaexpert.ru/PASSonline/index.php>) (Lagunin et al., 2000).

1) Receptor and test ligand preparation

The enzyme used had the code 5BQG with a resolution of 2.01 Å, and the inhibitor was the 2-Acylaminoimidazole molecule. Receptor preparation with the addition of hydrogen atoms and the removal of water molecules, and unused ligands was carried out using YASARA Structure software. Preparation of the test ligands using YASARA software involved minimizing bond energy by adding solvent molecules (water) into the system and then saving the file in *.pdb format (Aamir et al., 2018).

2) Ligand-receptor docking analysis with YASARA structure software

Molecular docking using YASARA structure software was studied. The prostaglandin receptor file with PDB code 5BQG as a result of preparation was stored in *.sce format until the best size was obtained at 1.0 Å to 5.0 Å 999 times. After validating the grid box size with a natural ligand redocking mechanism, the natural ligands were removed from the receptor and the file was saved in *.receptor.sce format. Then, the natural ligand from the bioavailability screening results in *.pdb format was input into the receptor structure and save it in *.complex.sce format. The docking process of the ligand-protein complex was carried out ten times until *.yob and *.txt files contained free energy values (ΔG), dissociation constants (kd), and amino acid residues (Gholam et al., 2024).

3) Prediction of bioavailability and toxicity

Bioavailability prediction was carried out to determine the permeability and solubility of a compound in the body. Bioavailability prediction was based on the Lipinski's rule of natural ligands. The Lipinski's rule includes molecular weights, hydrogen bond donors, hydrogen bond acceptors, log P and rotatable bonds. Ligands that have passed the Lipinski's rule are then measured for their toxicity. The criteria analyzed included carcinogenicity, acute oral toxicity (Lethal Dose 50/LD50), and Human Ether-A-Go-Go Related Gene (hERG). Both tests were carried out by entering the SMILES code (simplified molecular-input line-entry nine systems) owned by the test ligand into the pkCSM webserver (<http://biosig.unimelb.edu.au/pkcsml/>) (Nusantoro & Fadlan, 2020).

4) Data analysis

The docking results were analyzed using Excel by comparing the largest free energies, kd values, and interactions of amino acid residues. Docking result visualization involved tools like PyMol and Discovery Studio Visualizer to see 3D and 2D interactions (Gholam et al., 2024).

3. Results and Discussion

3.1 The yield of sungkai leaf extract

Yield is the ratio of the product's dry weight to the raw material's weight. The higher the yield value is obtained, the more bioactive components it contains. Dewatisari et al. (2018) reported that the yield value is related to plants' bioactive content. Based on the data presented in Table 1, the yield of sungkai leaf extract was 14.75%. The yield results were better than those obtained by Fadlilaturrahmah et al. (2021), who obtained 7.28% yield from ethanol extract.

Table 1. The yield of sungkai leaf extract in 70% ethanol solvent

Mass of Empty Container (g)	Container Mass + Sample (g)	Sample Mass (Paste) (g)	Initial Mass of Sample (simplisia) (g)	Moisture Content (%)	%Yield
86.27	87.59	1.34	10.00	10.8	14.75

The moisture content in foodstuffs greatly affects their quality and shelf life. Determination of the moisture content of a food ingredient is very important so that the processing and distribution process gets the right handling. Excessive moisture content can cause problems such as spoilage, microbial growth, degradation and reduced shelf life. Conversely, insufficient moisture content can cause brittleness, loss of texture, and decreased product quality (Prasetyo et al., 2019). Based on the research results, the moisture content of sungkai leaves was 10.8%. Utami et al. (2020) explained that the determination of moisture content is also related to the purity of the extract, where a moisture content that is too high (> 10%) can cause the growth of microbes that can reduce the stability of the extract. The results obtained in this study differ from similar studies; the differences may be caused by variation in the methods used during the research process.

3.2 Profiling of bioactive compounds in sungkai leaves using LC-MS

Bioactive profiling performed using the UPLC-QToF tool and the MassLynx application resulted in the identification of 22 known compounds and 1 unknown compound. The chromatogram reading was done by selecting one of the peaks and entering the molecular weight listed on the peak. After the molecular weight was entered, predictions appeared for several formulas that had the same molecular weight or slightly different one. The selection of compounds used the i-fit feature, which explained the percentage of similarities with the selected molecular weights. The identified compounds belonged to primary and secondary metabolite groups. Based on the data in Table 2, compound nos. 1, 3, and 4

were included in the alkaloid group because they had a heterocyclic structure with one or more nitrogen groups (Othman et al., 2019). Compound nos. 6, 9, 10, 11, 12, 13, 15, 17, 18, 19, and 22 belonged to the tannin group because they had a polyphenolic structure with uncharged nitrogen groups (Othman et al., 2019).

Compound no. 5 belonged to the phenolic group because it had a benzene ring that bound one or more hydroxyl groups (Lin et al., 2016). Compound no. 23 belonged to the carbohydrate group because it had carbon, hydrogen, and oxygen atoms. The basic molecular formula for carbohydrates is $(CH_2O)_n$ where n is at least 3 (Shailja & Singh, 2024). Compound nos. 8 and 20 belonged to the terpenoid group because they had simple linear hydrocarbon chains and complicated cyclic chains (Huang et al., 2021). Compound no. 16 belonged to the steroid group because it had three six-membered cyclohexane rings (rings A, B and C) and one five-membered cyclopentane ring (ring D) (Gomes et al., 2023). Compound no. 2 was included in the amino acid group because it consisted of a carboxylic group and an amine group linked by a peptide bond (Bischoff & Schlüter, 2012). Compound nos. 14 and 21 were included in the fatty acid group because they had a carboxylic group attached to a long carbon chain (Lund & Rustan, 2020).

Table 2. 2D class and structure of LC-MS compounds

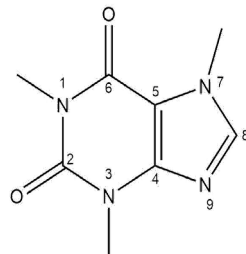
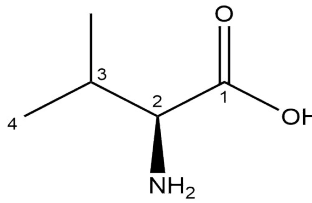
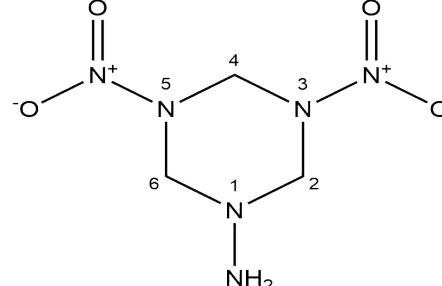
No	Formula	Mr	Compound Name (Class)	2D Structure
1	$C_8H_{10}N_4O_2$	194,191	Caffeine (Alkaloid)	
2	$C_5H_{11}NO_2$	117,146	L-(+)-Valine (Amino Acid)	
3	$C_3H_{10}N_6O_4^{+2}$	194,149	3,5-Dinitrohexahydro-1,3,5-triazine-1-amine (Alkaloid)	

Table 2. 2D class and structure of LC-MS compounds (continued)

No	Formula	Mr	Compound Name (Class)	2D Structure
4	C ₉ H ₁₂ N ₄ O ₄	240,216	1-Morpholin-4-yl-2-(4-nitro-pyrazol-1-yl)-ethanone (Alkaloid)	
5	C ₁₂ H ₁₄ O ₅	2,382,366	3,4,5-Trimethoxycinnamate (Phenolic)	
6	C ₁₆ H ₂₃ N ₄ O ₅ S ₂ Cl	450,961	(2S)-N-(5-chloro-1,3-thiazol-2-yl)-2-(4-methylsulfonyl-2-oxopiperazin-1-yl)-3-(oxan-2-yl)propenamide (Tanin)	
7	C ₁₄ H ₁₄ N ₁₂ OS	399,1212	Unknown	-
8	C ₂₉ H ₁₈ S	398,518	Thiophene, 2-(9,9'-spirobi[9H-fluoren]-2-yl)- (Terpene)	

Table 2. 2D class and structure of LC-MS compounds (continued)

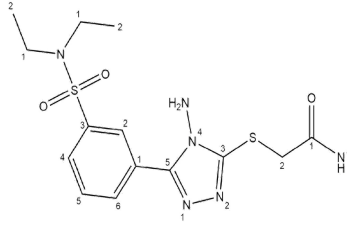
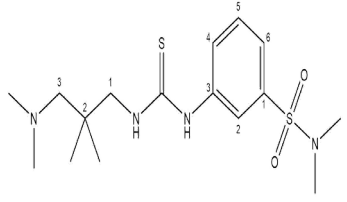
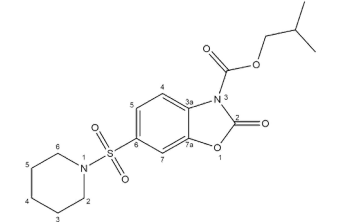
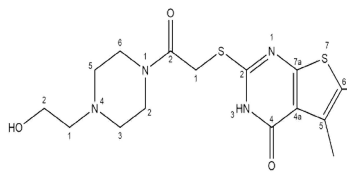
No	Formula	Mr	Compound Name (Class)	2D Structure
9	C ₁₅ H ₂₂ N ₆ O ₃ S ₂	398,504	2-({4-Amino-5-[3-(diethylsulfamoyl)phenyl]-4H-1,2,4-triazol-3-yl}sulfanyl)-N-methylacetamide (Tanin)	
10	C ₁₆ H ₂₈ N ₄ O ₂ S ₂	372,549	3-({[3-(Dimethylamino)-2,2-dimethylpropyl]carbamothioyl}amino)-N,N-dimethylbenzene sulfonamide (Tanin)	
11	C ₁₇ H ₂₂ N ₂ O ₆ S	382,431	2-Oxo-6-(piperidine-1-sulfonyl)-benzoxazole-3-carboxylic acid isobutyl ester (Tanin)	
12	C ₁₆ H ₂₂ N ₄ O ₃ S ₂	382,501	2-({2-[4-(2-Hydroxyethyl)-1-piperazinyl]-2-oxoethyl}sulfanyl)-5,6-dimethylthieno[2,3-d]pyrimidin-4(3H)-one (Tanin)	

Table 2. 2D class and structure of LC-MS compounds (continued)

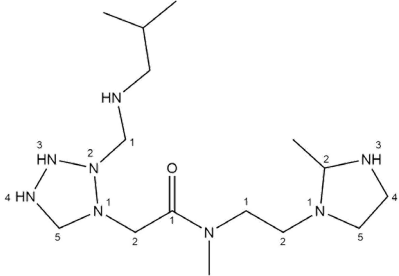
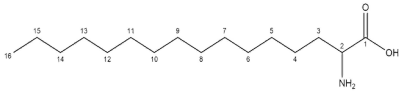
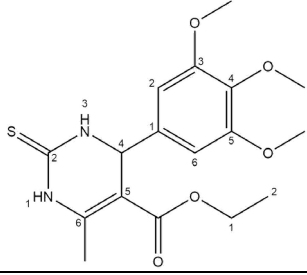
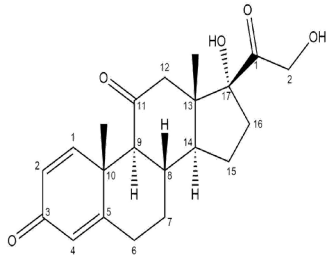
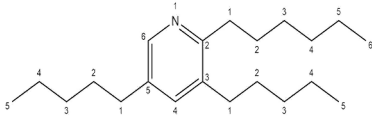
No	Formula	Mr	Compound Name (Class)	2D Structure
13	C ₁₅ H ₃₄ N ₈ O	342,483	2({[Isopropyl(methyl)amino]methyl}-1-tetrazolidinyl)-N-methyl-N-[2-(2-methyl-1-imidazolidinyl)ethyl]acetamide (Tanin)	
14	C ₁₆ H ₃₃ NO ₂	271,439	2-Aminopalmitic acid (Fatty Acid)	
15	C ₁₇ H ₂₂ N ₂ O ₅ S	366,432	Ethyl 6-methyl-2-thioxo-4-(3,4,5-trimethoxyphenyl)-1,2,3,4-tetrahydro-5-pyrimidinecarboxylate(Tanin)	
16	C ₂₁ H ₂₆ O ₅	358,428	Prednisone (Steroid)	
17	C ₂₁ H ₃₇ N	303,525	2-Hexyl-3,5-dipentylpyridine (Tanin)	

Table 2. 2D class and structure of LC-MS compounds (continued)

No	Formula	Mr	Compound Name (Class)	2D Structure
18	C ₁₃ H ₂₀ N ₂ O ₅ S	316,373	N-Isobutyl-N-[4-methoxyphenylsulfonyl]glycyl hydroxamic acid (Tanin)	
19	C ₁₉ H ₄₃ N ₇ O ₂	401,6	(2S)-2,6-diamino-N-[3-[3-[(2S)-2,6-diaminohexanoyl]amino]propyl-methylamino]propyl]hexanamide (Tanin)	
20	C ₃₇ H ₆₈ O ₄	576,933	2-Ethylhexyl 5-{8-[(2-ethylhexyl)oxy]-8-oxooctyl}-2-hexyl-3-cyclohexene-1-carboxylate (Terpene)	
21	C ₂₁ H ₃₈ O ₃	338,525	Glycidyl oleate (Fatty Acid)	
22	C ₄ H ₆ N ₁₀	194,157	5,5'-[(E)-1,2-Diazenediyl]bis(1-methyl-1H-tetrazole) (Tanin)	
23	C ₇ H ₁₄ O ₆	194,182	α-Methyl D-mannoside (Carbohydrate)	

3.3 Pharmacokinetic screening of sungkai leaf bioactive compounds based on the Lipinski's rule of 5

Pharmacokinetic screening can be carried out using the criteria established by Lipinski, which explains that the most "drug-like" molecules have a Log P value ≤ 5 , a molecular mass ≤ 500 , the number of hydrogen bond acceptors ≤ 10 , and the number of hydrogen bond donors ≤ 5 . Molecules that violate one/more of these regimens will have problems with bioavailability (Sahu et al., 2022). This is called the Lipinski's rule of 5 because the basic values are 5, 500, 2x5, and 5. The fifth and sixth rules describe the number of donors and acceptors of hydrogen bonds ≤ 12 and rotatable bonds ≤ 10 . The absorption of drugs in the human body starts from the intestinal epithelium to the blood and ends at the point of action of the drug. Previous research stated that compounds that have a mass of more than 500 daltons show absorption properties that are less than optimal (Sahu et al., 2022).

The data presented in Table 3 describes the range of molecular masses from 117.15 to 576.93 daltons. Drug candidates that violate these criteria tend to have low solubility and difficulty crossing cell membranes. Therefore, of the 22 compounds detected, only compound no. 19 showed low solubility and had difficulty crossing cell membranes. The second criterion is Log P, where the limit for lipophilicity is $\text{Log P} \leq 5$. Drug candidates that violate this criterion tend to be less soluble in physiological solutions, so they cannot access the membrane surface. The data presented in Table 3 shows that compound nos. 7, 16, 19, and 20 have a $\text{Log P} > 5$. If a compound is too hydrophobic ($\text{Log P} > 5$), the compound remains in the first membrane it contacts. If the compound is too hydrophilic, then the compound is unable to cross the cell membrane to arrive at the site of action. The number of hydrogen bond donors and acceptors is known to impact a molecule's physicochemical properties (solubility, absorption, distribution) and directly affect the efficacy of a drug. The rule of 5 states that for better absorption and permeability, the number of donors and acceptors in the ligand should be less than 5 and 10, respectively (Sahu et al., 2022). Based on Table 3, there are no compounds that violate this criterion. Sahu et al. (2022) explained that if a compound violates this criterion, then the compound is too polar to be able to pass through the cell membrane. Rotatable bonds are one non-ring bonded to a non-terminal (non-hydrogen) heavy atom. The C-N amide bond is not included because of the high rotational energy barrier (Sahu et al., 2022). This criterion demonstrates a good ability to determine the bioavailability of oral drugs. Bioavailability is the percentage of the dose successfully circulated in the body. Based on Table 3, compound nos. 13, 16, 18, 19, and 20 have rotatable bonds >10 , which causes the bioavailability of the four compounds to decrease. Topological polar surface areas of drug molecules have been reported to directly impact drug uptake across biological cell membranes such as those of colon carcinoma cells, and brain and nerve cells in the central nervous system. Karami et al. (2022) reported that drugs with dynamic TPSA $<60 \text{ \AA}^2$ can be completely absorbed, whereas drugs with TPSA $>140 \text{ \AA}^2$ have limited permeation. Based on Table 3, compound nos. 6, 7, 8, 9, 10, 11, 12, 14, 15, 19, and 20 have TPSA values $>140 \text{ \AA}^2$.

Table 3. Screening results of LC-MS compounds based on Lipinski's rule of 5

No	Compound Name	Lipinski's Rule of 5					
		Molecular Weight	Log P	Rotatable Bonds	Acceptors	Donors	Surface Area
1	Caffeine	194.19	-1.03	0	6	0	79.03
2	L-(+)-Valine	117.15	0.05	2	2	2	48.50
3	3,5-Dinitrohexahydro-1,3,5-triazine-1-amine	194.15	-2.18	2	4	3	72.30
4	1-Morpholin-4-yl-2-(4-nitro-pyrazol-1-yl)-ethanone	240.22	-0.35	3	6	0	96.91
5	3,4,5-Trimethoxycinnamate	238.24	1.81	5	4	1	99.23
6	2S)-N-(5-Chloro-1,3-thiazol-2-yl)-2-[4-(methylsulfonyl)-2-oxo-1-piperazinyl]-3-(tetrahydro-2H-pyran-2-yl)propanamide	450.97	1.17	6	7	1	172.59
7	Thiophene, 2-(9,9'-spirobi[9H-fluoren]-2-yl)-	398.53	7.76	1	1	0	179.65
8	2-({4-Amino-5-[3-(diethylsulfamoyl)phenyl]-4H-1,2,4-triazol-3-yl}sulfanyl)-N-methylacetamide	398.51	0.53	8	8	2	156.54
9	3-({[3-(Dimethylamino)-2,2-dimethylpropyl]carbamoithoyl} amino)-N,N-dimethylbenzenesulfonamide	372.56	1.81	7	4	2	150.82
10	2-Oxo-6-(piperidine-1-sulfonyl)-benzooxazole-3-carboxylic acid isobutyl ester	382.44	2.41	4	7	0	150.94
11	2-({2-[4-(2-Hydroxyethyl)-1-piperazinyl]-2-oxoethyl}sulfanyl)-5,6-dimethylthieno[2,3-d]pyrimidin-4(3H)-one	382.51	0.83	5	7	2	153.60

Table 3. Screening results of LC-MS compounds based on Lipinski's rule of 5 (continued)

No	Compound Name	Lipinski's Rule of 5					
		Molecular Weight	Log P	Rotatable Bonds	Acceptors	Donors	Surface Area
12	2-(5 {[Isopropyl(methyl) amino]methyl}-1-tetrazolidinyl)-N-methyl-N-[2-(2-methyl-1-imidazolidinyl)ethyl]acetamide	342.49	-1.81	8	8	4	145.15
13	2-Aminopalmitic acid	271.45	4.49	14	2	2	118.51
14	Ethyl 6-methyl-2-thioxo-4-(3,4,5-trimethoxyphenyl)-1,2,3,4-tetrahydro-5-pyrimidinecarboxylate	366.44	2.07	6	6	2	151.83
15	Prednisone	358.43	1.77	2	5	2	152.71
16	2-Hexyl-3,5-dipentylpyridine	303.53	6.67	13	1	0	138.49
17	N-Isobutyl-N-[4-methoxyphenylsulfonyl]glycyl hydroxamic acid	316.38	0.85	7	5	2	124.08
18	(2S)-2,6-diamino-N-[3-[3-[(2S)-2,6-diaminohexanoyl]amino]propyl-methylamino]propyl]hexanamide	313.45	-0.90	13	5	4	133.71
19	2-Ethylhexyl 5-{8-[(2-ethylhexyl)oxy]-8-oxooctyl}-2-hexyl-3-cyclohexene-1-carboxylate	576.93	11.02	26	4	0	254.73
20	glycidyl oleate	338.53	5.97	17	3	0	148.73
21	5,5'-[(E)-1,2-Diazenediyl]bis(1-methyl-1H-tetrazole)	194.16	-0.85	2	10	0	77.63
22	α -Methyl D-mannoside	194.18	-2.57	2	6	4	75.33

Description: Red color indicates the compound violates one/more of the Lipinski's rule of 5

3.4 ADMET-based screening of sungkai leaf bioactive compounds

ADMET (absorption, distribution, metabolism, excretion, and toxicity) is a set of criteria that has a role in the assessment of pharmacokinetic and pharmacodynamic effects of drug molecules. The calculation of ADMET properties is very important in optimizing new drug molecules. Successful drug development must involve good ADMET properties in addition to good efficacy. *In silico* methods have been introduced into drug discovery and development as a tool capable of predicting the ADMET properties of drugs at an early stage (Chandrasekaran et al., 2018). ADMET data is considered critical in the discovery and development of new drugs. Both *in vitro* and *in vivo* model testing provide criteria for the properties of ADMET drugs, which can be used to predict drug properties after administration. The ADMET criteria determine if a drug candidate can pass further testing, or it should be detained or discontinued. Preclinical data on ADMET properties display that the drug plays a role in assessing drug targeting after administration because the pharmacokinetic profile can be based on ADMET drug data. Parameters including the rate of drug absorption, deposition, and metabolism in the targeted organs are considered when assessing drug exposure at the target site of action (Chandrasekaran et al., 2018). The intestine is the first site for the absorption of orally administered drugs. Compounds are defined in terms of absorption percentage through the human intestine. Molecules with less than 30% absorbance are considered to be difficult to absorb (Pires et al., 2015). Based on the data presented in Table 4, the intestinal absorption range of compounds that passed the Lipinski's rule of 5 screening ranged from 44.091 to 100%. Thus, all compounds successfully met these criteria and could be absorbed by the intestine. The blood-brain barrier (BBB) criterion is the ability to allow blood vessels to vascularize the central nervous system (CNS), which strictly regulates the movement of ions, molecules and cells between the blood and the brain (Nusantoro & Fadlan, 2020). The BBB protects the brain from exogenous compounds. The ability of a drug to enter the brain is an important criterion to be considered to help reduce side effects and toxicity or to increase the efficacy of drugs acting in the brain. The BBB is calculated *in vivo* in animal models in units of logBB, the logarithmic ratio of the brain drug concentration to plasma. If a compound has a logBB > 0.3, it can cross the BBB, while molecules with a logBB < -1 are less able to distribute it in the brain (Pires et al., 2015). Based on Table 4, compound nos. 6, 10, 11, and 21 have logBB values < -1. This shows that these four compounds can be less distributed in the brain.

The Ames test is a widely used technique for testing the mutagenic ability of a compound using bacteria and a positive result indicates that the compound is mutagenic. Therefore, the compounds that failed this test can be carcinogens (Pires et al., 2015). Based on Table 4, the compounds with positive Ames toxicity results were compound nos. 3, 4, 6, 14, 15, 17, and 21. The hERG inhibitor criteria I and II suggest that inhibition of the potassium channel encoded by the hERG (human ether-a-go-go gene) is the principal cause of the development of QT syndrome – which causes dangerous ventricular arrhythmias. HERG channel inhibition has led to the withdrawal of many substances from the drug market (Pires et al., 2015). Based on Table 4, compound nos. 7 and 9 fail to meet this criterion, so they are considered compounds harmful when consumed by humans. Toxicity potential is very important for potential compounds.

Table 4. Screening results of LC-MS compound findings based on ADMET

No	Compound Name	ADMET					
		Intestinal Absorption	BBB	AMES	hERG I	hERG II	LD50
1	Caffeine	98.81	-0.25	No	No	No	3.04
2	L-(+)-Valine	77.22	-0.38	No	No	No	1.59
3	3,5-Dinitrohexahydro-1,3,5-triazine-1-amine	64.22	-0.9	Yes	No	No	2.4
4	1-Morpholin-4-yl-2-(4-nitro-pyrazol-1-yl)-ethanone	88.79	-0.75	Yes	No	No	2.28
5	3,4,5-Trimethoxycinnamate	97.59	-0.52	No	No	No	2.56
6	2S)-N-(5-Chloro-1,3-thiazol-2-yl)-2-[4-(methylsulfonyl)-2-oxo-1-piperazinyl]-3-(tetrahydro-2H-pyran-2-yl)propanamide	77.35	-1.41	Yes	No	No	3.41
7	Thiophene, 2-(9,9'-spirobi[9H-fluoren]-2-yl)-	100	1.32	No	No	Yes	2.16
8	2-({4-Amino-5-[3-(diethylsulfamoyl)phenyl]-4H-1,2,4-triazol-3-yl}sulfanyl)-N-methylacetamide	79.7	-0.79	No	No	No	2.32
9	3-({[3-(Dimethylamino)-2,2-dimethylpropyl]carbamoithiyl} amino)-N,N-dimethylbenzenesulfonamide	92.36	0.03	No	No	Yes	2.53
10	2-Oxo-6-(piperidine-1-sulfonyl)-benzooxazole-3-carboxylic acid isobutyl ester	94.54	-1.12	No	No	No	2.92
11	2-({2-[4-(2-Hydroxyethyl)-1-piperazinyl]-2-oxoethyl}sulfanyl)-5,6-dimethylthieno[2,3-d]pyrimidin-4(3H)-one	67.52	-1.08	No	No	No	1.8
12	2-(5 {[Isopropyl(methyl) amino]methyl}-1-tetrazolidinyl)-N-methyl-N-[2-(2-methyl-1-imidazolidinyl)ethyl]acetamide	50.36	-0.08	No	No	No	2.25

Table 4. Screening results of LC-MS compound findings based on ADMET (continued)

No	Compound Name	ADMET					
		Intestinal Absorption	BBB	AMES	hERG I	hERG II	LD50
13	2-Aminopalmitic acid	89.83	-0.37	No	No	No	2.25
14	Ethyl 6-methyl-2-thioxo-4-(3,4,5-trimethoxyphenyl)-1,2,3,4-tetrahydro-5-pyrimidinecarboxylate	93.21	-0.59	Yes	No	No	2.83
15	Prednisone	82.84	-0.02	Yes	No	No	1.94
16	2-Hexyl-3,5-dipentylpyridine	91.48	0.99	No	No	No	1.82
17	N-Isobutyl-N-[4-methoxyphenylsulfonyl]glycyl hydroxamic acid	67.63	-0.96	Yes	No	No	2.32
18	(2S)-2,6-diamino-N-[3-[3-[(2S)-2,6-diaminohexanoyl]amino]propyl-methylamino]propyl]hexanamide	44.09	-0.75	No	No	No	1.98
19	2-Ethylhexyl 5-{8-[(2-ethylhexyl)oxy]-8-oxooctyl}-2-hexyl-3-cyclohexene-1-carboxylate	89.06	-0.37	No	No	No	1.5
20	glycidyl oleate	93.1	-0.48	No	No	No	1.67
21	5,5'-[(E)-1,2-Diazenediyl]bis(1-methyl-1H-tetrazole)	86.93	-1.39	Yes	No	No	3.02
22	α-Methyl D-mannoside	48.28	-0.73	No	No	No	1.28

Description: Compounds that fail to meet AMES/hERG I/hERG II criteria are declared **DANGEROUS** if consumed by humans

Lethal dosage value (LD50) is a standard measure of acute toxicity to assess the relative toxicity of other known molecules from database. LD50 values mean that the compound tested can directly cause the death of 50% of the test animals. Based on the explanation from Government of British Columbia (2022), acute toxicity is divided into three categories: High (less than 500 mg/kg body weight), moderate (500-1000 mg/kg body weight), and low (1000-2000 mg/kg body weight). Based on Table 4, compounds that fell into the high category are compound nos. 2, 3, and 22. Compounds that fell into the moderate category are compound nos. 1, 4, 5, 7, 8, 9, 11, 12, 13, 15, 16, 17, 18, 19, 20, and 21. Compound nos. 6, 10, 14 are in the low category. Based on the screening results, compounds that pass the rule of 5 and ADMET screening will be tethered with the target enzyme, mPGES-1.

3.5 Grid box and molecular docking validation with mPGES-1 target enzyme

Grid box validation uses the YASARA structure program to re-attach the natural ligand to the receptor. The validation function is used to obtain a grid box size that can cover the active side of mPGES-1. The results of the validation in Table 5 show that 1.5Å had the lowest root mean square deviation (RMSD) value among the grid boxes 1 Å - 5 Å with a value of 1.1106 Å. RMSD describes the deviation of ligand poses between the 3D crystallographic structures and the results of re-docking. Flexible ligands can affect the precision of the position of the complex formed. RMSD values close to zero indicate the suitability of the ligand pose of the re-pinching result. Grid box sizes can be used in virtual screening processes with RMSD values ≤ 2 Å (Irsal et al., 2022).

The inhibition constant is proportional to the binding energy value; the greater the inhibition constant, the higher the free energy value, and vice versa. The binding energy values and dissociation constants obtained by each ligand are affected by the interaction between the ligand and the receptor (Maulana et al., 2022). The Gibbs free energy describes the ability of the test ligand to form stable complexes with enzymes or receptors. Gibbs free energy is a thermodynamic parameter that can determine chemical reactions based on changes in enthalpy (ΔH) and entropy (ΔS) at a certain pressure and temperature. The more negative the ΔG value, the more stable and spontaneous the drug is, so the bond between the ligand and the acceptor is stable and strong (Irsal et al., 2022). The best compound was obtained after ten compounds passed the screening and were successfully anchored with mPGES-1. Table 6 shows that compound nos. 5, 7, 6, 4 and 3 were the five compounds with the highest binding energies. In addition to the compounds from the screening results, the binding energy value of the drug compound acetaminophen was also obtained. Based on Table 3, the five best compounds had greater binding energy values than acetaminophen. This explains that these compounds were better able to inhibit the mPGES-1 enzyme and thus reduce fever faster.

Table 5. The RMSD of gridbox used in mPGES-1 molecular docking

Natural Ligand Name	RMSD on Size (Angstrom)								
	1.0 Å	1.5 Å	2.0 Å	2.5 Å	3.0 Å	3.5 Å	4.0 Å	4.5 Å	5.0 Å
4UJ (ligand-ligand)	2.03	1.93	2.01	2.03	2.02	2.01	2.04	2.01	2.01
4UJ (protein-protein)	1.12	1.11	1.11	1.12	1.11	1.11	1.12	1.11	1.11

Table 6. Virtual screening of ligands that passed Lipinski's rule of 5 and ADMET

No	Ligand Name	Binding Energy (kcal/mol)	Dissoc. Eonstant (μ M)	Inhibition Constant (μ M)	% Abundance	Retention Time
1	Caffeine	3.42	3.12	3.1	0.02	0.7
2	L-(+)-Valine	3.5	2.72	2.71	0.39	1.26
3	3,4,5-Trimethoxycinnamate	4.09	1.01	1	0.06	5.25 and 5.68
4	2-({4-Amino-5-[3-(diethyl	4.33	0.68	0.67	0.08	8.55
5	sulfamoyl)phenyl]-4H-1,2,4-triazol-3- yl)sulfanyl)-N-methyl	5.08	0.19	0.19	5.93	9.37 and 11.10
6	acetamide	4.45	0.55	0.54	0.93	9.74
7	2-Oxo-6-(piperidine-1-sulfonyl)- benzooxazole-3-carboxylic	4.8	0.3	0.3	0.35	10.22
8	acid isobutyl ester	3.86	1.49	1.48	0.6	10.75
9	2-({2-[4-(2-Hydroxyethyl)-1-piperaziny]-2- oxoethyl)sulfanyl)-5,6-dimethylthieno[2,3- d]pyrimidin-4(3H)-one	3.45	2.97	2.95	0.25	13.98
10	2-(5-{[Isopropyl(methyl)amino]	3.37	3.42	3.39	0	21.97
11	methyl]-1-tetrazolidinyl)-N-methyl N-[2-(2- methyl-1-imidazolidinyl)ethyl]acetamide	3.55	2.52	2.5	-	-

Description: Acetaminophen is a drug ligand used as a virtual *screening* reference for ligands that pass the test. If the ligand performs better than acetaminophen, it is more efficient at inhibiting the mPGES-1 enzyme.

3.6 2D and 3D visualization of amino acid interaction results of molecular docking

Docking analysis explains how the compound is anchored in the receptor and interacts with important residues, both polar and non-polar. Based on the data in Table 7, 4UJ, the natural docked ligand, has conventional hydrogen bond interaction with ASN74 and hydrophobic Pi-Pi stacked interaction with TYR130. The interactions are visualized in Figure 1. Compound no. 3 has hydrogen bond interaction with HIS113 and ARG126, and hydrophobic pi-alkyl interaction with TYR130. Compound no. 4 has conventional hydrogen bond interaction with ARG73 and SER127, hydrophobic Pi-Pi stacked interaction with TYR130, and alkyl interaction with VAL128. Compound no. 5 has a conventional hydrogen bond interaction with ARG126, hydrophobic alkyl bonds with ARG126 and VAL 128 residues, and pi-alkyl bond interaction with HIS113 and ARG128. The interactions are visualized in Figure 2.

Compound no. 6 has conventional hydrogen bond interactions with ARG126 and SER127, carbon-hydrogen bond interaction with SER127, hydrophobic pi-alkyl bonds with HIS113 and TYR130 residues, and Pi-Pi stacked bond interaction with TYR130. Compound no. 7 has conventional hydrogen bond interaction with ASN74, ARG126, and SER127 and carbon-hydrogen bond interaction with SER127. Compound no. 23, acetaminophene, has a conventional hydrogen bond interaction with ASN 74 and hydrophobic Pi-Pi stacked interaction with TYR 130. The interactions are visualized in Figure 3.

Table 7. Residues involved in the interaction between ligands and the enzyme mPGES-1

Ligand	Residues/Amino acids Involved	
	Hydrophobic Interaction	Hydrogen Bond
4UJ (Natural Ligand)	A TYR 130	A SER 127
3,4,5-Trimethoxycinnamate(Compound 3)	A TYR 130	A HIS 113, A ARG 126
2-({4-Amino-5-[3-(diethylsulfamoyl)phenyl]-4H-1,2,4-triazol-3-yl}sulfanyl)-N-methylacetamide(Compound 4)	A VAL 128, A TYR 130	A ARG 73, A SER 127
2-Oxo-6-(piperidine-1-sulfonyl)-benzoxazole-3-carboxylic acid isobutyl ester(Compound 5)	A HIS 113, A VAL 128, A TYR 130	A ARG 126
2-({2-[4-(2-Hydroxyethyl)-1-piperazinyl]-2-oxoethyl}sulfanyl)-5,6-dimethylthieno[2,3-d]pyrimidin-4(3H)-one(Compound 6)	A HIS 113, A TYR 130	A ARG 126, A SER 127
2-(5-{[Isopropyl(methyl)amino]methyl}-1-tetrazolidinyl)-N-methyl-N-[2-(2-methyl-1-imidazolidinyl)ethyl]acetamide (Compound 7)		A ASN74, A ARG126, A SER127
Acetaminophen (Comparison ligands)		A ASN 74

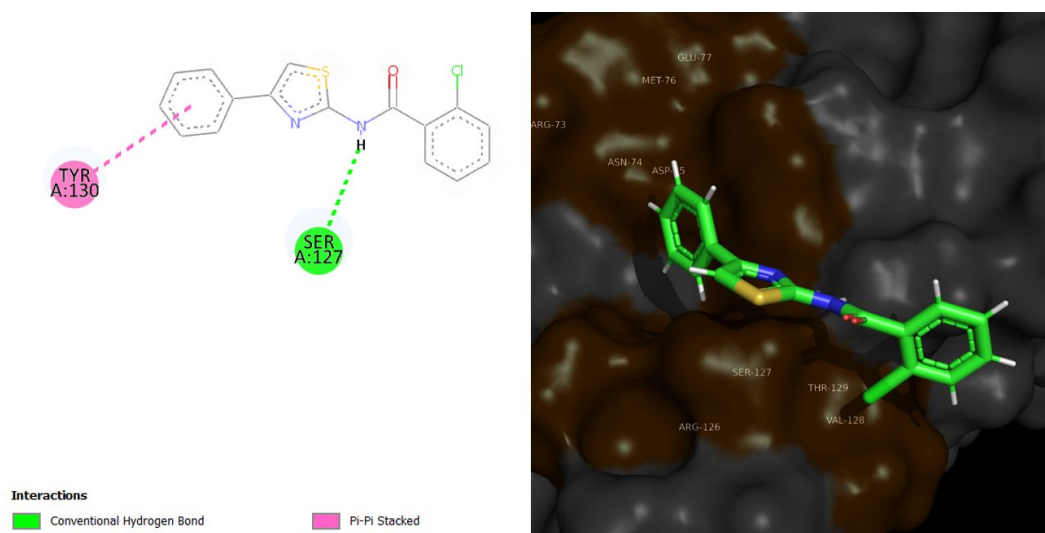


Figure 1. 2D visualization and 3D visualization of 4UJ interaction with mPGES-1

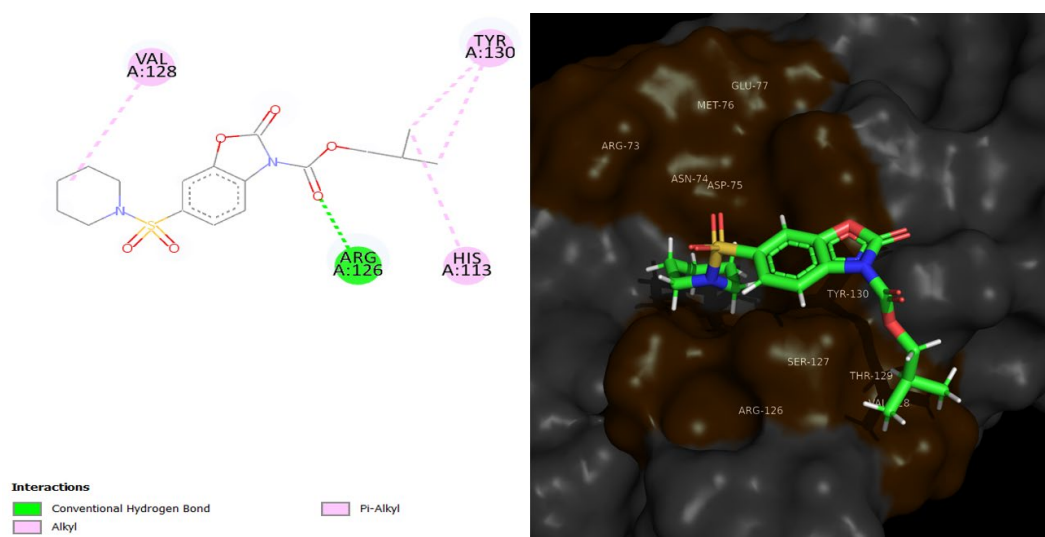


Figure 2. 2D visualization and 3D visualization of compound 5 interaction with mPGES-1

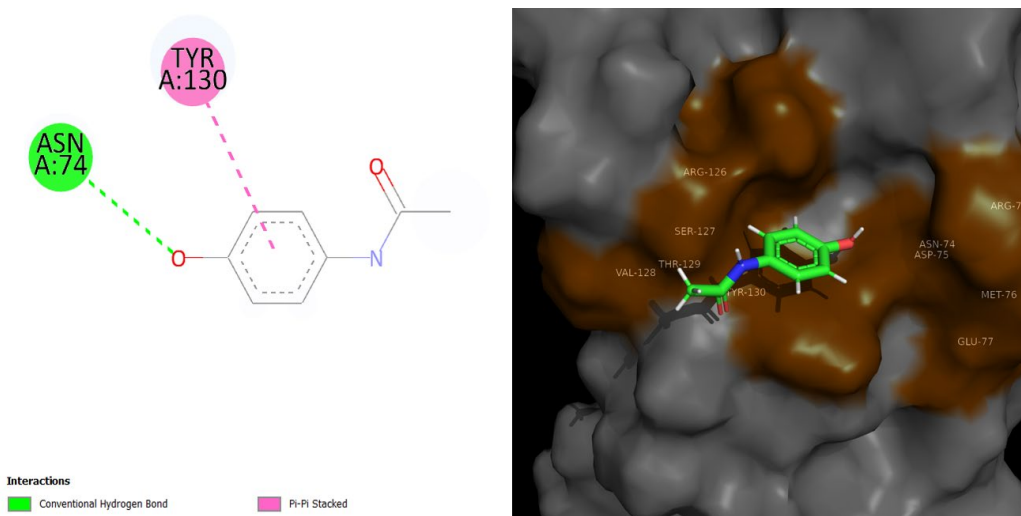


Figure 3. 2D visualization and 3D visualization of acetaminophen interaction with mPGES-1

4. Conclusions

Sungkai leaf extraction gave a yield of 14.75%. LC-MS results showed the presence of 22 known metabolites and one unknown compound. After screening using parameters from Lipinski's rule of 5 and ADMET, ten compounds that passed the screening were obtained. The binding results with the target enzyme mPGES-1 showed that the compounds 2-oxo-6-(piperidine-1-sulfonyl)-benzoxazole-3-carboxylic acid isobutyl ester; 2-(5-[[Isopropyl (methyl) amino]methyl]-1-tetrazolidinyl)-N-methyl N-[2-(2-methyl-1-imidazolidinyl)ethyl] acetamide; 2-({2-[4-(2-Hydroxyethyl)-1-piperazinyl]-2-oxoethyl}sulfanyl)-5,6-dimethylthieno [2,3-d] pyrimidin-4(3H)-one; 2-({4-Amino-5-[3-(diethylsulfamoyl)phenyl]-4H-1,2,4-triazol-3-yl} sulfanyl)-N-methyl Acetamide; and 3,4,5-trimethoxycinnamate had better mPGES-1 inhibitory activity than the drug compounds (acetaminophen/paracetamol) in terms of the binding energy and inhibition constant of each tested ligand.

5. Acknowledgements

The author would like to thank all parties who have helped complete this research. All authors made equal contributions as the main contributors to this manuscript paper. No funding resource was reported for this publication.

6. Conflicts of Interest

All authors declare there is no conflict of interest regarding this publication.

ORCID

Muhammad Marsha Azzami Hasibuan <https://orcid.org/0009-0000-8110-6672>

Dimas Andrianto <https://orcid.org/0000-0003-4406-5810>

R. Haryo Bimo Setiarto <https://orcid.org/0000-0001-6894-7119>

References

- Aamir, M., Singh, V. K., Dubey, M. K., Meena, M., Kashyap, S. P., Katari, S. K., Upadhyay, R. S., Umamaheswari, A., & Singh, S. (2018). In silico prediction, characterization, molecular docking, and dynamic studies on fungal SDRs as novel targets for searching potential fungicides against Fusarium wilt in tomatoes. *Frontiers in Pharmacology*, 9, Article 1038. <https://doi.org/10.3389/fphar.2018.01038>
- Bischoff, R., & Schlüter, H. (2012). Amino acids: Chemistry, functionality and selected non-enzymatic post-translational modifications. *Journal of Proteomics*, 75(8), 2275-2296. <https://doi.org/10.1016/j.jprot.2012.01.041>
- Carlson, C., Kurnia, B., & Widodo, A. D. (2019). Tatalaksana terkini demam pada anak. *Jurnal Kedokteran Meditek*, 24(67), 43-51. <https://doi.org/10.36452/jkdoktmeditek.v24i67.1684>
- Chandrasekaran, B., Abed, S. N., Al-Attraqchi, O., Kuche, K., & Tekade, R. K. (2018). Computer-aided prediction of pharmacokinetic (ADMET) properties. In R. K. Tekade (Ed.). *Dosage form design parameters* (Vol. 2, pp. 731-755). Elsevier. <https://doi.org/10.1016/B978-0-12-814421-3.00021-X>
- Dewatisari, W. F., Rumiyan, L., & Rakhmawati, I. (2018). Rendemen dan skrining fitokimia pada ekstrak daun Sansevieria sp. *Jurnal Penelitian Pertanian Terapan*, 17(3), 197-202. <https://doi.org/10.25181/jppt.v17i3.336>
- Fadlilaturrahmah, F., Putra, A. M. P., Rizki, M. I., & Nor, T. (2021). Uji aktivitas antioksidan dan antitirozinase fraksi n-Butanol daun sungkai (*Peronema canescens* Jack.) secara kualitatif menggunakan kromatografi lapis tipis. *Jurnal Pharmascience*, 8(2), 90-101. <https://doi.org/10.20527/jps.v8i2.11160>
- Gholam, G. M., Irsal, R. A. P., Dwicesaria, M. A., & Hasibuan, M. M. A. (2024). In silico study of combined docking and molecular dynamics simulation for hops (*Humulus lupulus*) active compounds in inhibiting Duffy-binding protein (DBP) as anti-*Plasmodium vivax* (P. vivax). *Proceedings*, 103(1), Article 66. <https://doi.org/10.3390/proceedings2024103066>
- Gomes, A. R., Pires, A. S., Roleira, F. M. F., & Tavares-da-Silva, E. J. (2023). The structural diversity and biological activity of steroid oximes. *Molecules*, 28(4), Article 1690. <https://doi.org/10.3390/molecules28041690>
- Government of British Columbia. (2022). *Pesticide toxicity and hazard*. <https://www2.gov.bc.ca/assets/gov/farming-natural-resources-and-industry/agriculture-and-seafood/animal-and-crops/plant-health/pesticide-toxicity-hazard.pdf>
- Hanafi, H., Irawan, C., Rochaeni, H., Sulistiawaty, L., Roziafanto, A. N., & Supriyono. (2018). Phytochemical screening, LC-MS studies and antidiabetic potential of methanol extracts of seed shells of *Archidendron bubalinum* (Jack) I.C. Nielson (Julang Jaling) from Lampung, Indonesia. *Pharmacognosy Journal*, 10(6), S77-S82. <https://doi.org/10.5530/pj.2018.6s.15>
- Huang, J., Yang, L., Zou, Y., Luo, S., Wang, X., Liang, Y., Du, Y., Feng, R., & Wei, Q. (2021). Antibacterial activity and mechanism of three isomeric terpineols of *Cinnamomum longepaniculatum* leaf oil. *Folia Microbiologica*, 66(1), 59-67. <https://doi.org/10.1007/s12223-020-00818-0>
- Irsal, R. A. P., Hami Seno, D. S., Safithri, M., & Kurniasih, R. (2022). Penapisan virtual senyawa aktif sirih merah (*Piper crocatum*) sebagai inhibitor Angiotensin Converting Enzyme. *Jurnal Farmamedika (Pharmamedica Journal)*, 7(2), 104-113. <https://doi.org/10.47219/ath.v7i2.157>
- Karami, T. K., Hailu, S., Feng, S., Graham, R., & Gukasyan, H. J. (2022). Eyes on Lipinski's rule of five: a new "rule of thumb" for physicochemical design space of ophthalmic

- drugs. *Journal of Ocular Pharmacology and Therapeutics*, 38(1), 43-55. <https://doi.org/10.1089/jop.2021.0069>
- Lagunin, A., Stepanchikova, A., Filimonov, D., & Poroikov, V. (2000). PASS: Prediction of activity spectra for biologically active substances. *Bioinformatics*, 16(8), 747-748. <https://doi.org/10.1093/bioinformatics/16.8.747>
- Latief, M., Tarigan, I. L., Sari, P. M., & Aurora, F. E. (2021). Aktivitas antihiperurisemia ekstrak etanol daun sungkai (*Peronema canescens* Jack) pada mencit putih jantan. *Pharmacon: Jurnal Farmasi Indonesia*, 18(1), 23-37. <https://doi.org/10.23917/pharmacon.v18i01.12880>
- Lin, D., Xiao, M., Zhao, J., Li, Z., Xing, B., Li, X., Kong, M., Li, L., Zhang, Q., Liu, Y., Chen, H., Qin, W., Wu, H., & Chen, S. (2016). An overview of plant phenolic compounds and their importance in human nutrition and management of type 2 diabetes. *Molecules*, 21(10), Article 1374. <https://doi.org/10.3390/molecules21101374>
- Lund, J., & Rustan, A. C. (2020). Fatty acids: Structures and properties. In *Encyclopedia of Life Sciences* (Issue October, pp. 283-292). Wiley. <https://doi.org/10.1002/9780470015902.a0029198>
- Maulana, F., Muhammad, A. A., Umar, A., Mahendra, F. R., Musthofa, M., & Nurcholis, W. (2022). Profiling metabolites through chemometric analysis in *Orthosiphon aristatus* extracts as α -glucosidase inhibitory activity and in silico molecular docking. *Indonesian Journal of Chemistry*, 22(2), 501-514. <https://doi.org/10.22146/ijc.71334>
- Nusantoro, Y. R., & Fadlan, A. (2020). Analisis sifat mirip obat, prediksi ADMET, dan penambatan molekular Isatinil-2-Aminobenzoilhidrazon dan kompleks logam transisi Co(II), Ni(II), Cu(II), Zn(II) terhadap BCL2-XL. *Akta Kimia Indonesia*, 5(2), 114-126. <https://doi.org/10.12962/j25493736.v5i2.7881>
- Othman, L., Sleiman, A., & Abdel-Massih, R. M. (2019). Antimicrobial activity of polyphenols and alkaloids in middle eastern plants. *Frontiers in Microbiology*, 10, Article 911. <https://doi.org/10.3389/fmicb.2019.00911>
- Pindan, N. P., Daniel, Saleh, C., & Magdaleni, A. R. (2021). Uji fitokimia dan uji aktivitas antioksidan ekstrak fraksi n-heksana, etil asetat dan etanol sisa dari daun sungkai (*Peronema canescens* Jack.) dengan metode DPPH. *Jurnal Atomik*, 6(1), 22-27.
- Pires, D. E. V., Blundell, T. L., & Ascher, D. B. (2015). pkCSM: Predicting small-molecule pharmacokinetic and toxicity properties using graph-based signatures. *Journal of Medicinal Chemistry*, 58(9), 4066-4072. <https://doi.org/10.1021/acs.jmedchem.5b00104>
- Prasetyo, T. F., Isdiana, A. F., & Sujadi, H. (2019). Implementasi alat pendeteksi kadar air pada bahan pangan berbasis internet of things. *SMARTICS Journal*, 5(2), 81-96. <https://doi.org/10.21067/smartics.v5i2.3700>
- Rafita, I. D., Lisdiana, & Marianti, A. (2016). Pengaruh ekstrak kayu manis terhadap gambaran histopatologi dan kadar sgot-sgpt hepar tikus yang diinduksi parasetamol. *Unnes Journal of Life Science*, 4(1), 29-37.
- Sahu, V. K., Singh, R. K., & Singh, P. P. (2022). Extended rule of five and prediction of biological activity of peptidic HIV-1-PR inhibitors. *Universal Journal of Pharmacy and Pharmacology*, 1(1), 20-42. <https://doi.org/10.31586/ujpp.2022.403>
- Shailja, & Singh, P. (2024). Carbohydrate Structure and Role. *International Journal of Multidisciplinary Research & Reviews*, 3(2), 52-72. <https://doi.org/10.56815/ijmrr.v3i2.2024/52-72>
- Sharma, C. V., & Mehta, V. (2014). Paracetamol: Mechanisms and updates. Continuing Education in Anaesthesia. *Critical Care and Pain*, 14(4), 153-158. <https://doi.org/10.1093/bjaceaccp/mkt049>
- Utami, Y. P., Sisang, S., & Burhan, A. (2020). Pengukuran parameter simplisia dan ekstrak etanol daun patikala (*Etlingera elatior* (Jack) R.M. Sm) asal Kabupaten Enrekang

- Sulawesi Selatan. *Majalah Farmasi dan Farmakologi*, 24(1), 5-10.
<https://doi.org/10.20956/mff.v24i1.9831>
- Walter, E. J., Hanna-Jumma, S., Carraretto, M., & Forni, L. (2016). The pathophysiological basis and consequences of fever. *Critical Care*, 20(1), Article 200.
<https://doi.org/10.1186/s13054-016-1375-5>
- Yani, A. P., Ruyani, A., Yenita, Ansyori, I., & Irwanto, R. (2014). Uji potensi daun muda sungkai (*Peronema canescens*) untuk kesehatan (imunitas) pada mencit (*Mus musculus*). [The potential test of sungkai young leaves (*Peronema canescens*) to maintain good health (immunity) in mice (*Mus musculus*)]. *Prosiding Seminar Nasional XI Biologi*, 11(1), 245-250.